

# On the dynamic stabilization of an inverted pendulum

Eugene I. Butikov<sup>a)</sup>

*St. Petersburg State University, St. Petersburg, Russia*

(Received 21 June 2000; accepted 19 January 2001)

A simple qualitative physical explanation is suggested for the phenomenon of dynamic stabilization of the inverted rigid planar pendulum whose pivot is constrained to oscillate with a high frequency in the vertical direction. A quantitative theory based on the suggested approach is developed. A computer program simulating the physical system supports the analytical investigation. The simulation reveals subtle details of the motion and aids the analytical study of the subject in a manner that is mutually reinforcing. © 2001 American Association of Physics Teachers.  
[DOI: 10.1119/1.1365403]

## I. INTRODUCTION: THE PHYSICAL SYSTEM

An ordinary rigid planar pendulum suspended in the uniform gravitational field is a very useful and versatile physical model famous first of all for its outstanding role in the history of physics. The pendulum is also interesting as a paradigm of contemporary nonlinear physics and, more importantly, because the differential equation of the pendulum is frequently encountered in various branches of modern physics. For example, the mathematical relationships associated with the limiting motion of a frictionless pendulum, i.e., the motion with the total energy that equals the potential energy in the inverted position (this motion delimits swinging from rotation in a full circle, see, e.g., Ref. 1), play an important role in the theory of solitons, in the problem of super-radiation in quantum optics, and in the theory of Josephson effects in weak superconductivity. Thus, the pendulum is a rather simple classic nonlinear mechanical device which models many physical systems. Mechanical analogies can be very useful in gaining an intuitive understanding of complex phenomena.

Various kinds of motion of the pendulum whose axis is driven periodically in the vertical direction are of special interest. Depending on the frequency and amplitude of this constrained oscillation of the suspension point, this seemingly simple system exhibits a rich variety of nonlinear phenomena characterized by amazingly different types of motion. Some modes of such a parametrically forced pendulum are quite simple indeed and agree well with our intuition, while others are very complicated and counterintuitive.

When the external frequency is approximately twice the natural frequency of the pendulum, the lower state of equilibrium becomes unstable, and the system leaves it, executing oscillations whose amplitude increases progressively, provided the driving amplitude exceeds some threshold value. This phenomenon is called parametric resonance. In contrast to the case of ordinary resonance caused by a direct influence of some periodic external force, over the threshold friction is unable to restrict the growth of parametrically excited oscillations. The growth of the amplitude is restricted because the period of natural oscillations increases with the amplitude due to nonlinear properties of the pendulum: The resonance conditions, being fulfilled for small amplitudes, become violated as the amplitude increases. Parametric resonance is possible when two driving cycles occur during approximately one, two, three, and any other integer number of natural periods. With increasing friction, parametric resonances of higher orders become weaker and disappear.

Another possible kind of regular motion is a synchronized nonuniform unidirectional rotation in a full circle with a period that equals either the period of the constrained motion of the axis or an integer multiple of this period. More complicated regular modes of the parametrically forced pendulum are formed by combined rotational and oscillating motions synchronized (locked in phase) with oscillations of the pivot. Different competing modes can coexist at the same values of the driving amplitude and frequency. Which mode is activated depends on the starting conditions.

The behavior of the pendulum whose axis is forced to oscillate with a frequency from a certain interval (and with large enough amplitude) can be irregular, chaotic. The pendulum makes several revolutions in one direction, then swings for a while with permanently changing amplitude, then rotates again in the former or in the opposite direction, and so forth. For other values of the driving frequency and/or amplitude, the chaotic motion can be purely oscillatory, without revolutions. The pendulum can make, say, one oscillation during each of two driving periods, but in each next cycle the motion (the phase orbit) is slightly (and randomly) different from the previous cycle. At first sight such essentially unpredictable, random behavior contradicts the well-known uniqueness of solution to a differential equation of motion with given initial conditions. Within the scope of classical mechanics which naturally includes the concept of mechanical determinism, chaotic behavior of simple dynamical systems is considered admissible only as a result of external random perturbations of the system, i.e., as something introduced from the outside, from the environment. The discovery of random behavior and intrinsic irregular, chaotic oscillations in deterministic dynamical systems of different nature (physical, chemical, biological) is one of the most prominent recent scientific sensations. It is remarkable that such a simple mechanical system as a pendulum whose pivot is forced to oscillate regularly can exhibit under some conditions a chaotic behavior, illustrated by a strange attractor in the phase plane. Chaotic modes of the parametrically driven pendulum have been intensively investigated over the past decades.<sup>2-7</sup>

Another well-known interesting feature in the behavior of a rigid pendulum whose suspension point is constrained to vibrate with a high frequency along the vertical line is the dynamic stabilization of its inverted position. When the frequency and/or the amplitude of these vibrations are large enough (the necessary conditions are determined in the following), the inverted pendulum shows no tendency to turn down. Moreover, at small and moderate deviations from the

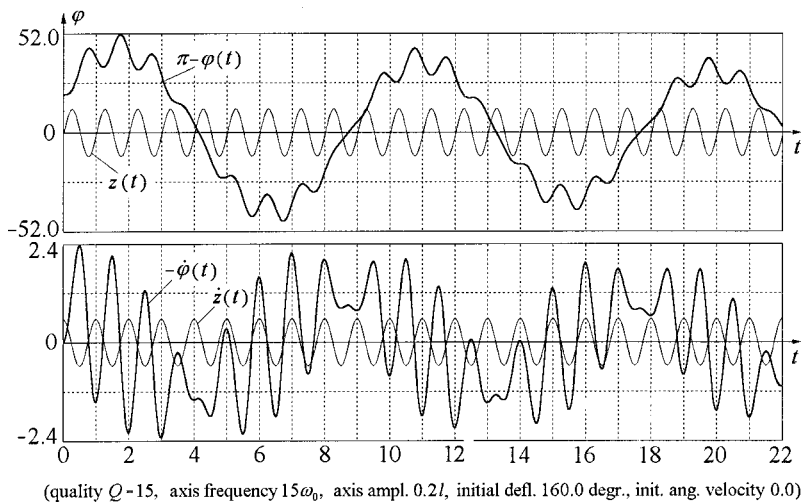


Fig. 1. Graphs of the angular deflection from the inverted (upside-down) position and of the angular velocity for the pendulum whose axis is oscillating with a high frequency. The graphs are obtained by a numerical integration of the exact differential equation for the momentary angular deflection  $\varphi(t)$ , Eq. (11).

vertical inverted position the pendulum tends to return to it. Being deviated, it can execute relatively slow oscillations about the vertical line on the background of rapid oscillations of the suspension point. An example of the graphs of such oscillations of the inverted pendulum obtained in the computer simulation of the motion is shown in Fig. 1. We note how the rapid vibrations superimpose on the slow oscillation and distort its smooth shape. In the presence of friction these slow oscillations gradually damp away, and the pendulum eventually comes to the vertical inverted position.

This type of dynamic stability probably was first pointed out by Stephenson almost a century ago.<sup>8</sup> In 1951 such extraordinary behavior of the pendulum was explained and investigated experimentally in detail by Pjotr Kapitza,<sup>9</sup> and the corresponding physical device is now widely known in Russia as “Kapitza’s pendulum.” Simple hand-made devices are often used to show in lectures this fascinating phenomenon of classical mechanics. An old electric shaver’s mechanism can serve perfectly well to force the pivot of a light rigid pendulum vibrating with a high enough frequency and sufficient amplitude to make the inverted position stable. Such demonstrations inevitably evoke a vivid response and some kind of bewilderment, perplexing and even astonishing those students who see it for the first time.

After Kapitza, this simple but very curious and intriguing system attracted the attention of many researchers, and the theory of the phenomenon may seem to be well elaborated (see, e.g., Ref. 10). Nevertheless, more and more new features in the behavior of this apparently inexhaustible system are reported regularly. Many related papers have been published in recent years in the American Journal of Physics.<sup>11–20</sup>

However, in the abundant literature on the subject (a vast bibliography can be found in Ref. 21) the author failed to discover a simple and clear interpretation of this interesting phenomenon. Understanding the dynamic stabilization of an inverted pendulum is certainly a challenge to our intuition. The principal aim of this paper is to present a quite simple qualitative physical explanation of the phenomenon. We focus also on an approximate quantitative theory (leading to the well-known concept of the effective potential for the slow motion of the pendulum) which can be developed on the basis of the suggested approach to the problem. Finally, we show that the loss of dynamic stability at large ampli-

tudes of the pivot is closely related to the commonly known conditions of parametric instability of the noninverted pendulum.

## II. PHYSICAL REASONS FOR STABILITY OF THE INVERTED PENDULUM WHOSE PIVOT IS OSCILLATING AT HIGH FREQUENCY

For simplicity we consider a light rigid rod of length  $l$  with a heavy small bob of mass  $m$  on its end and assume that the rod has zero mass, so that all the mass of the pendulum is concentrated in the bob. The force of gravity  $mg$  provides a restoring torque  $-mgl \sin \varphi$  whose value is proportional to the sine of angular deflection  $\varphi$  of the pendulum from the equilibrium position. With the suspension point at rest, this torque makes the deviated pendulum swing about the lower stable equilibrium position. When the axis of the pendulum is constrained to move with acceleration along the vertical line, it is convenient to analyze the motion in the noninertial reference frame associated with this axis. Doing so, we must imply that due to the acceleration of this frame of reference there is one more force exerted on the pendulum, namely the force of inertia  $-m\ddot{z}$ , where  $z(t)$  is the time-dependent vertical coordinate of the axis. The torque of this force  $-m\ddot{z}l \sin \varphi$  must be added to the torque of the gravitational force.

Let the axis of the pendulum be forced to execute a given harmonic oscillation along the vertical line with a frequency  $\omega$  and an amplitude  $a$ , i.e., let the constrained motion of the axis be described by

$$z(t) = a \sin \omega t. \quad (1)$$

The force of inertia  $F_{\text{in}}(t)$  exerted on the bob in the non-inertial frame of reference also has a sinusoidal dependence on time:

$$F_{\text{in}}(t) = -m\ddot{z}(t) = ma\omega^2 \sin \omega t. \quad (2)$$

This force of inertia is directed downward during the time intervals for which  $z(t) = a \sin \omega t < 0$ , i.e. when the axis is below the middle point of its oscillations. We see this directly from the equation for  $F_{\text{in}}(t)$ , Eq. (2), whose right-hand side depends on time as  $\sin \omega t$ , that is, exactly as the  $z$  coordinate of the axis [see Eq. (1)]. Therefore during the corre-

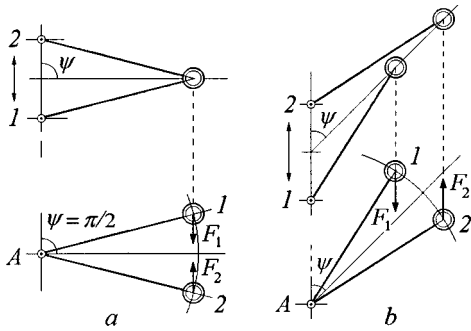


Fig. 2. The forces of inertia exerted on the pendulum in the noninertial reference frame at the extreme positions 1 and 2 of the oscillating axis  $A$ .

sponding half-period of the oscillation of the pivot, this additional force is equivalent to some strengthening of the force of gravity. During the other half-period the axis is above its middle position ( $z(t) = a \sin \omega t > 0$ ), and the action of this additional force is equivalent to some weakening of the gravitational force. When the frequency and/or amplitude of the pivot are large enough (when  $a\omega^2 > g$ ), for some part of the period the apparent gravity is even directed upward.

On the basis of this approach, taking into account the periodic variations of the apparent gravity, we can easily explain, say, the physical reason for the ordinary parametric swinging of the pendulum when its pivot is driven vertically with a frequency approximately twice the frequency of natural oscillations.

In the case of rapid oscillations of the axis, the mean value of the force of inertia, averaged over the short period of these oscillations, is zero, but the value of its *torque* averaged over the period about the axis is not zero. Next we show why. This nonzero mean torque of the force of inertia explains the pendulum stabilization in the inverted position.

Let us begin with the case in which the rod of the pendulum is oriented horizontally, i.e., at the right angle  $\psi = \pi/2$  to the direction of oscillations of the axis [Fig. 2(a)].

To better understand the influence of the force of inertia upon the system, we first forget for a while about the force of gravity. (Explaining the phenomenon in lectures, it is possible to “switch off” gravity for a while simply by changing the orientation of the vibrating device mentioned earlier, so that the pendulum’s axis of rotation is vertical. Then the rigid pendulum occurs in a state of indifferent equilibrium at any orientation in the horizontal plane until the axis is vibrating.) If the bob has zero initial velocity, in the inertial reference frame in the absence of gravity it stays practically at the same level while the axis  $A$  oscillates between the extreme points 1 and 2 and the rod turns down and up through a small angle, as shown in the upper part of Fig. 2(a). In the noninertial frame of reference associated with the oscillating axis, the same motion of the rod is shown in the lower part of Fig. 2(a): The bob of the pendulum moves up and down along an arc of a circle and occurs in positions 1 and 2 [the lower part of Fig. 2(a)] at the instants at which the oscillating axis reaches its extreme positions 1 and 2, respectively [the upper part of Fig. 2(a)]. In position 1 the force of inertia  $F_1$  exerted on the bob is directed downward, and in position 2 the force  $F_2$  of the same magnitude is directed upward. The arm of the force in positions 1 and 2 is the same, therefore the torque of this force, averaged over the period of oscillations, is zero. In the absence of gravity this orientation of the pendulum (per-

pendicularly to the direction of oscillations) corresponds to a dynamic equilibrium position (an unstable one, as we shall see later).

Now let us consider the case in which on average the rod is deflected through an arbitrary angle  $\psi$  from the direction of oscillations, and the axis oscillates between extreme points 1 and 2, as shown in the upper part of Fig. 2(b). In the noninertial frame of reference associated with the oscillating axis, the bob moves at these oscillations between points 1 and 2 in the lower part of Fig. 2(b) along an arc of a circle whose center coincides with the axis  $A$  of the pendulum. We note that the rod has the same simultaneous orientations in both reference frames at instant 1 as well as at instant 2. When the axis is displaced downward (to position 1) from its midpoint, the force of inertia  $F_1$  exerted on the bob is also directed downward. In the other extreme position 2 the force of inertia  $F_2$  has an equal magnitude and is directed upward. However, now the torque of the force of inertia in position 2 is greater than in position 1 because the *arm* of the force in this position is greater. Therefore on average the force of inertia creates a torque about the axis that tends to turn the pendulum upward, into the vertical inverted position, in which the rod is parallel to the direction of oscillations. Certainly, if the pendulum makes an acute angle with respect to the downward vertical position, the mean torque of the force of inertia tends to turn the pendulum downward.

Thus, the torque of the force of inertia, averaged over a period of oscillations, tends to align the pendulum along the direction of constrained oscillations of the axis. The right-hand side (b) of Fig. 2 presents an utterly simple and clear explanation to the origin of this torque. Kapitza<sup>9</sup> called this torque *vibrational*, but we can also call it *inertial*, because its origin is related to the force of inertia that arises due to the constrained rapid vibrations of the axis. For given values of the driving frequency and amplitude, this torque depends only on the angle of the pendulum’s deflection from the direction of the pivot’s vibration. This mean inertial torque does not depend on time explicitly, and its influence on the pendulum can be considered exactly in the same way as the influence of other ordinary external torques, such as the torque of the gravitational force. The inertial torque gives the desired explanation for the physical reason of existence of the two stable equilibrium positions that correspond to the two preferable orientations of the pendulum’s rod along the direction of the pivot’s vibration. With gravity, the inverted pendulum is stable with respect to small deviations from this position provided the mean torque of the force of inertia is greater than the torque of the force of gravity.

### III. AN APPROXIMATE QUANTITATIVE THEORY OF THE INVERTED PENDULUM

Now we can determine the quantitative conditions, which provide the dynamic stabilization of the inverted equilibrium position in the presence of the force of gravity. Rapid vertical vibrations of the axis make the inverted position stable if at small deflections from this position the torque of the force of inertia, averaged over the period of rapid oscillations (this torque tends to return the pendulum to the inverted position), is greater in magnitude than the torque of the gravitational force that tends to tip the pendulum down.

We can consider the motion of the pendulum whose axis is vibrating with a high frequency as a superposition of two components: a “slow” or “smooth” component, whose

variation during a period of constrained vibrations is small, and a “fast” (or “vibrational”) component. Let’s imagine an observer who doesn’t notice (or doesn’t want to notice) the vibrational component of this compound motion. If this observer uses, for example, a stroboscopic illumination with a short interval between the flashes that equals the period of constrained vibrations of the pendulum’s axis, he/she can see only the slow component of the motion. Our principal interest is to determine this slow component.

When the rod of the pendulum is deflected from the downward vertical position on the average through an angle  $\psi$ , the instantaneous value  $\varphi(t)$  of the deflection angle is subjected to an additional rapid almost sinusoidal oscillation with the frequency  $\omega$  about this average value  $\psi = \langle \varphi(t) \rangle$  because of the constrained oscillation of the axis. This can be clearly seen from the plots of the angular deflection and velocity (Fig. 1). Therefore we can try to search for the instantaneous angle of deflection  $\varphi(t)$  as the sum of a slowly varying function  $\psi(t) = \langle \varphi(t) \rangle$  and a fast term  $\delta(t)$  whose mean value is zero. This additional angle  $\delta(t)$  oscillates with the high frequency  $\omega$  with an amplitude proportional to the sine of the momentary value of  $\psi(t)$ :

$$\begin{aligned}\varphi(t) &= \psi(t) + \delta(t) = \psi(t) - \frac{z(t)}{l} \sin \psi \\ &= \psi(t) - \frac{a}{l} \sin \psi \sin \omega t.\end{aligned}\quad (3)$$

Here  $a$  is the amplitude of forced vibrations of the axis and  $l$  is the length of the pendulum. (When the axis is over its middle position,  $z$  is positive and the additional angle  $\delta = -(z/l)\sin \psi$  is negative, if  $\psi > 0$ .) Later on we shall find the differential equation for this unknown slowly varying function  $\psi(t)$  that describes the smooth motion of the pendulum, averaged over the period of rapid oscillations.

The torque of the force of inertia depends on the momentary value of this force  $ma\omega^2 \sin \omega t$ , Eq. (2), and on the sine of the angle  $\varphi$ . The oscillations of the axis cause only small deviations of the momentary deflection angle  $\varphi$  from its average value  $\psi$  (i.e.,  $\delta(t) \ll 1$  for all  $t$ ), and so for the sine of the deflection angle we can write the following approximate expression:

$$\sin \varphi = \sin(\psi + \delta) \approx \sin \psi + \delta \cos \psi.\quad (4)$$

With the help of this equation, we can find the approximate value of the gravitational torque about the point of suspension (about the axis of the pendulum), averaged over the period of rapid oscillations of the axis:

$$\langle -mgl \sin \varphi \rangle = -mgl \langle \sin(\psi + \delta) \rangle = -mgl \sin \psi,\quad (5)$$

because the average value of  $\delta(t)$  is zero:  $\langle \delta(t) \rangle = 0$ . We see that the mean torque of the gravitational force is the same as in the case of a pendulum with the immovable suspension point: The oscillating second term in the expansion for the momentary angle, Eq. (4), being multiplied by a constant gravitational force, gives no contribution to the mean torque. However, when we take the time average for the torque of the oscillating force of inertia, the first term in the expansion (4) vanishes, but the oscillating second term gives a nonzero contribution. This occurs by virtue of the identical sinusoidal dependence on time both of the force of inertia  $F_{\text{in}}(t)$  given

by Eq. (2) and of  $\delta(t)$  whose value determines the oscillating arm of this force:

$$\begin{aligned}\langle F_{\text{in}}(t)l \sin(\psi + \delta) \rangle &= -ma\omega^2 l(a/l) \cos \psi \sin \psi \langle \sin^2 \omega t \rangle \\ &= -\frac{1}{2}ma^2\omega^2 \cos \psi \sin \psi,\end{aligned}\quad (6)$$

because the average value of the sine squared equals  $1/2$ :  $\langle \sin^2 \omega t \rangle = 1/2$ . For  $\psi > \pi/2$  the average value of the torque of the force of inertia is positive: If the pendulum makes an acute angle with the upward vertical direction, this torque tends to turn the pendulum up. Comparing the right-hand sides of Eqs. (5) and (6), we see that the torque of the force of inertia can exceed in magnitude the torque of the gravitational force tending to tip the pendulum down, when the following condition is fulfilled:

$$a^2\omega^2 > 2gl.\quad (7)$$

Thus, the inverted position of the pendulum is stable if the maximal velocity  $\omega a$  of the vibrating axis is greater than the velocity  $\sqrt{2gl}$  attained by a body during a free fall from the height that equals the pendulum length  $l$ . We can write this criterion of stability in another form, using the expression  $\omega_0^2 = g/l$  for the frequency  $\omega_0$  of small natural oscillations of the pendulum in the absence of forced vibrations of the axis. Substituting  $g = l\omega_0^2$  in Eq. (7) we get

$$\frac{a}{l} \frac{\omega}{\omega_0} > \sqrt{2}.\quad (8)$$

According to Eq. (8), the product of the dimensionless normalized amplitude of forced oscillations of the axis  $a/l$  and the dimensionless (normalized) frequency of these oscillations  $\omega/\omega_0$  must exceed the square root of 2. For instance, for the pendulum whose length  $l = 20$  cm and the frequency of forced oscillations of the axis  $f = \omega/2\pi = 100$  Hz, the amplitude  $a$  must be greater than 3.2 mm. To provide the dynamic stabilization of the inverted pendulum within some finite interval of the angles of deflection from the vertical position, the product of the normalized amplitude of forced oscillations of the axis and the normalized frequency must be greater than  $\sqrt{2}$  by a finite value. For a physical pendulum, the condition of dynamic stability in the inverted position is expressed by the same equation (7) or (8) provided we imply by the quantity  $l$  the reduced length of the pendulum  $I/md$ , where  $I$  is the moment of inertia with respect to the axis of rotation,  $m$  is the mass, and  $d$  is the distance between the axis and the center of mass. We note that the criterion (7) or (8) is independent of friction.

The critical minimum value of the product of the driving amplitude and frequency  $a\omega$  found above, Eq. (8), agrees with the lower boundary of stability of the inverted pendulum obtained by approximating the exact nonlinear equation of motion by the Mathieu equation, the solutions of which are widely documented in the extensive literature concerning the problem (see, e.g., Ref. 11, 12, or 13). However, the investigation based on the Mathieu equation and infinite Hill’s determinants gives little physical insight into the problem and, more importantly, is restricted to motion within small angles from the vertical. On the contrary, the above explanation clearly shows the physical reason for the dynamic stabilization of the inverted pendulum and is free from the restriction of small angles.

In particular, on the basis of the approach developed in this paper, for given values of the frequency  $\omega$  and amplitude

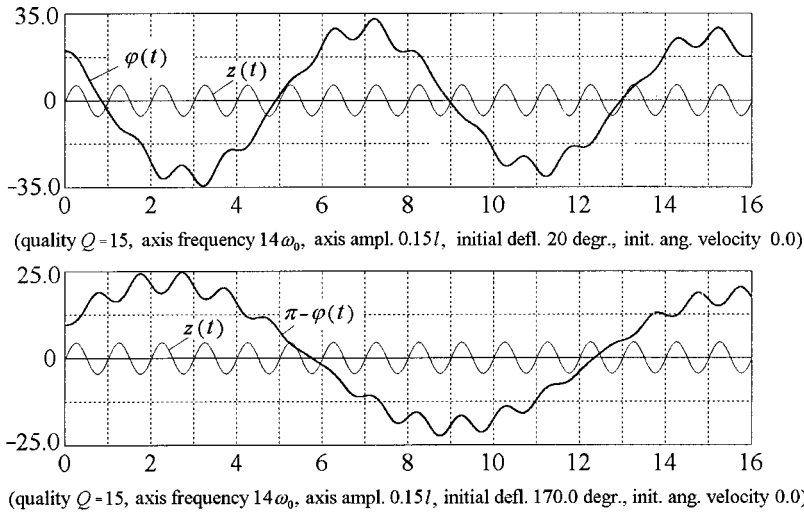


Fig. 3. The graphs of oscillations of the pendulum about the lower and upper equilibrium positions, respectively. The graphs are obtained by a numerical integration of the exact differential equation for the momentary angular deflection  $\varphi(t)$ , Eq. (11).

$a$  of forced oscillations of the axis, we can find the maximal admissible angular deflection from the inverted vertical position  $\theta_{\max} = \pi - \psi_0$  for which the pendulum will return to this position, even when  $\theta_{\max}$  is almost as large as  $\pi/2$ . To do this, we should equate the right-hand sides of Eqs. (5) and (6) that determine the average values of the torque of the gravitational force which tends to tip the pendulum down and of the torque of the force of inertia which tends to return the pendulum to the inverted position:

$$\cos \theta_{\max} = -\cos \psi_0 = \frac{2gl}{a^2 \omega^2} = 2 \left( \frac{\omega_0 l}{\omega a} \right)^2. \quad (9)$$

This expression for an admissible angular excursion from the inverted equilibrium position is valid for arbitrarily large values of  $\theta$ . The greater the product of the frequency and the amplitude  $\omega a$  of constrained vibrations of the axis, the closer the angle  $\theta_{\max}$  to  $\pi/2$ . Being deflected from the vertical position by an angle that does not exceed  $\theta_{\max}$ , the pendulum will execute relatively slow oscillations about this inverted position. This slow motion occurs both under the mean torque of the force of inertia and the force of gravity. Rapid oscillations with the frequency of forced vibrations of the axis superimpose on this slow motion of the pendulum. With friction, the slow motion gradually damps, and the pendulum wobbles up settling eventually in the inverted position.

Similar behavior of the pendulum can be observed when it is deflected from the lower vertical position. But in this case the frequency of slow oscillations is greater than for the inverted pendulum. Indeed, for the hanging down pendulum the averaged torque of the force of inertia tends to return the pendulum to the lower vertical position together with the torque of the gravitational force. Therefore the frequency of these slow oscillations is greater than both the frequency of slow oscillations in the absence of gravity and the frequency of natural oscillations in the absence of forced vibrations of the axis. The clock with a pendulum subjected to a fast vertical vibration will always be ahead of time. The frequencies  $\omega_{\text{up}}$  and  $\omega_{\text{down}}$  of small slow oscillations about the inverted position and the lower vertical position are given by

$$\omega_{\text{up}}^2 = \frac{a^2 \omega^2}{2l^2} - \omega_0^2, \quad \omega_{\text{down}}^2 = \frac{a^2 \omega^2}{2l^2} + \omega_0^2. \quad (10)$$

If we put  $\omega_0 = 0$  into these formulas, we get the expression  $\omega_{\text{slow}} = a/(l\sqrt{2})\omega$  for the frequency of small slow oscillations of the pendulum with vibrating axis in the absence of the gravitational force. These oscillations can occur about either of the two equivalent stable equilibrium positions located opposite one another along the direction of forced vibrations of the axis. For vertical vibrations of the axis in the field of gravity, the force of gravity increases the average restoring torque of the force of inertia (and consequently the frequency of slow oscillations) about the lower equilibrium position, and the force of gravity decreases the average restoring torque (and hence the frequency of slow oscillations) about the upper equilibrium position. We can illustrate these results concerning the periods of slow oscillations about the two vertical positions with the graphs in Fig. 3, obtained in a simulation experiment on the computer.

The simulation is based on a numerical integration of the exact differential equation for the momentary angular deflection  $\varphi(t)$ . This equation includes, besides the torque of the force of gravity, the instantaneous (not averaged over the fast period) value of the torque exerted on the pendulum by the force of inertia that depends explicitly on time  $t$ :

$$\ddot{\varphi} + 2\gamma\dot{\varphi} + \omega_0^2 \left( 1 - \frac{a}{l} \frac{\omega^2}{\omega_0^2} \sin \omega t \right) \sin \varphi = 0. \quad (11)$$

The second term takes into account the braking frictional torque, assumed to be proportional to the momentary angular velocity  $\dot{\varphi}$  in the mathematical model of the simulated system. The damping constant  $\gamma$  is related to the dimensionless quality factor  $Q$  characterizing the role of viscous friction:  $Q = \omega_0/2\gamma$ .

It is worth mentioning that the results of this section concerning the smooth behavior of the pendulum with a rapidly vibrating axis are found without the differential equation for the system under consideration. Being obtained by a decomposition of motion on slow oscillations and rapid vibrations with the driving frequency, these results are approximate and valid when the amplitude of constrained vibration of the axis is small compared to the pendulum's length ( $a \ll l$ ). Moreover, in the presence of gravity the driving frequency must be much greater than the frequency of small natural oscillations of the pendulum ( $\omega \gg \omega_0$ ). These restrictions mean that

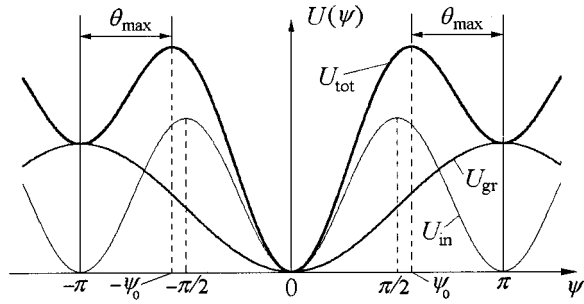


Fig. 4. Graphs of the gravitational potential energy  $U_{\text{gr}}$ , mean potential energy  $U_{\text{in}}$  in the field of the force of inertia, and of the total potential energy  $U_{\text{tot}}(\psi)$  for the pendulum with an oscillating axis.

we should not expect from the approach discussed here to give an exhaustive description of the parametrically driven pendulum in all cases.

In particular, within certain ranges of the system parameters (in the intervals of parametric instability) the lower position of the pendulum becomes unstable, as we already mentioned earlier. However, parametric resonance, as well as the modes of chaotic behavior, occurs at such driving frequencies (for the principal parametric resonance  $\omega \approx 2\omega_0$ ) that do not satisfy the conditions of applicability of the approach used above. Therefore we cannot require from this approach an explanation of chaotic modes and parametric instability of the noninverted pendulum. This approach predicts well the lower bound of the stability of the inverted pendulum, but does not yield the upper bound, which is closely related to ordinary parametric resonance of the non-inverted pendulum (see Sec. VII).

#### IV. EFFECTIVE POTENTIAL FUNCTION FOR A PENDULUM WITH THE AXIS VIBRATING AT HIGH FREQUENCY

The approximate differential equation for the slow motion of the pendulum can be written under the assumption that the angular acceleration  $\ddot{\psi}(t)$  in this slow motion is determined by the mean torque  $N(\psi)$  exerted on the pendulum in the noninertial frame of reference associated with its axis:

$$\ddot{\psi} = -\omega_0^2 \sin \psi - \frac{1}{2} \frac{a^2}{l^2} \omega^2 \cos \psi \sin \psi. \quad (12)$$

The mean torque on the right-hand side of Eq. (12) is calculated approximately under the assumption that the slowly varying angular coordinate  $\psi(t)$  is “frozen.” To facilitate interpretation of the slow motion described by this nonlinear differential equation, we can introduce a potential function  $U(\psi)$  that corresponds to the mean torque  $N(\psi)$  exerted on the pendulum. The torque is determined by the derivative of this potential function:  $N(\psi) = -dU(\psi)/d\psi$ . The observer mentioned earlier who doesn’t notice the rapid oscillating motion of the pendulum can simply consider that the system moves in an effective potential field  $U = U(\psi)$ . Such a potential function that governs the smooth motion of the pendulum averaged over the rapid oscillations was first introduced by Landau,<sup>10</sup> and derived by various different methods afterwards (see, e.g., Ref. 16, 19, or 20). From the right-hand part of Eq. (12) we conclude that the effective

potential consists of two parts  $U_{\text{gr}}(\psi)$  and  $U_{\text{in}}(\psi)$  describing the influence of the force of gravity and the force of inertia, respectively:

$$U(\psi) = U_{\text{gr}}(\psi) + U_{\text{in}}(\psi) \\ = mgl(1 - \cos \psi) + \frac{1}{4} ma^2 \omega^2 (1 - \cos 2\psi). \quad (13)$$

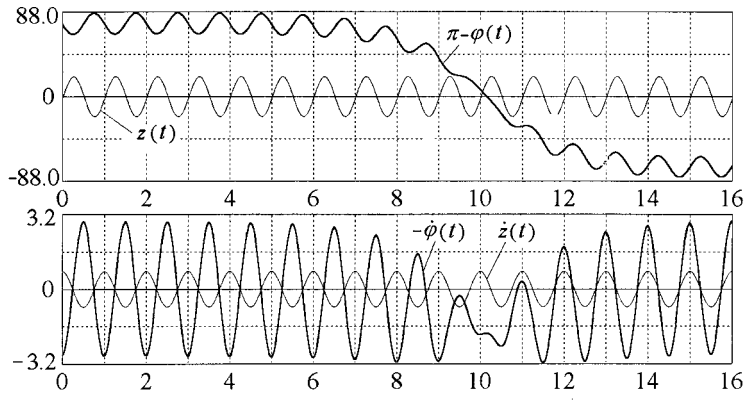
The graphs of  $U_{\text{gr}}(\psi)$  and  $U_{\text{in}}(\psi)$  are shown in Fig. 4. They both have a sinusoidal shape, but the period of  $U_{\text{in}}(\psi)$  is just one half of the period of  $U_{\text{gr}}(\psi)$ . Their minima at  $\psi = 0$  coincide, thus generating the principal minimum of the total potential function  $U(\psi) = U_{\text{tot}}(\psi)$ . This minimum corresponds to the stable lower equilibrium position of the pendulum. But the next minimum of  $U_{\text{in}}(\psi)$  is located at  $\psi = \pi$ , where  $U_{\text{gr}}(\psi)$  has its maximum corresponding to the inverted position of the pendulum.

If criterion (7) or (8) is fulfilled, the amplitude of  $U_{\text{in}}(\psi)$  is greater than that of  $U_{\text{gr}}(\psi)$ . Then the potential function  $U(\psi)$  has (in addition to the absolute minimum at  $\psi = 0$  which corresponds to the lower equilibrium position) relative minima at  $\psi = \pm\pi$ . Both additional minima correspond to the same inverted position of the pendulum. Oscillations of a particle trapped in an additional minimum describe the behavior of the inverted pendulum. Slow small oscillations occurring near the bottom of a potential well are almost harmonic. The slopes of the shallow additional potential wells are not as steep as the slopes of the principal well at  $\psi = 0$ . Therefore the frequency  $\omega_{\text{up}}$  of slow small oscillations about the inverted position is smaller than the frequency  $\omega_{\text{down}}$  of small oscillations within the principal well (about the lower vertical position), in accordance with the expressions obtained earlier (10) and with the simulations represented by the graphs in Fig. 3. Certainly, some subtle details in the motion of the pendulum revealed by the simulations are lost in our approximate analysis, which refers only to the slow component of the investigated motion. Nevertheless, this analysis allows us to clearly interpret principal features of the physical system under consideration.

The maxima of the total potential energy  $U(\psi)$  are determined by Eq. (9). The tops of the potential barrier between the two wells occur at deflections  $\pm\psi_0$  ( $\psi_0 > \pi/2$ ) from the lower vertical position and  $\pm\theta_{\text{max}}$  ( $\theta_{\text{max}} < \pi/2$ ) from the upper equilibrium position (Fig. 4). At these positions of the pendulum, the mean torque of gravity is balanced by the mean torque of the force of inertia. However, these equilibrium positions are unstable: The slightest disturbance makes the pendulum slowly slip down into one of the wells and oscillate there moving from one slope to the other and back. The pattern of such slow oscillations (averaged over the fast period of constrained vibrations) is far from a sine curve. The pendulum stays for a prolonged time near the summit of the potential barrier at the utmost deflection, and then moves rather fast toward the other utmost deflection to linger there again before the backward fast motion. The simulation of such a motion is shown in Fig. 5.

#### V. THE PENDULUM WITH A HORIZONTALLY VIBRATING PIVOT

A similar approach can be applied to the pendulum whose axis is forced to rapidly oscillate in the horizontal direction. In this case the force of inertia  $F_{\text{in}}(t) = -m\ddot{x}(t)$  is directed horizontally. Its mean torque tends to align the pendulum



(quality  $Q=300$ , axis frequency  $15\omega_0$ , axis ampl.  $0.2l$ , initial defl.  $104$  degr., init. ang. velocity  $2.8425$ )

Fig. 5. The graphs of oscillations of the pendulum about the inverted position with maximal possible angular excursion. The graphs are obtained by a numerical integration of the exact differential equation for the momentary angular deflection  $\varphi(t)$ , Eq. (11).

horizontally, repelling it both from downward and inverted vertical positions. The torque is determined by an expression of the opposite sign compared with the similar Eq. (6) for the vertical vibration:

$$\langle F_{in}(t)l \cos(\psi + \delta) \rangle = \frac{1}{2}ma^2\omega^2 \cos \psi \sin \psi. \quad (14)$$

In the absence of gravitation this torque creates two stable equilibrium positions located oppositely (at  $\psi = \pm \pi/2$ ) on the same level with the axis. The force of gravity deviates downward these symmetrical equilibrium positions.

The graphs of potential functions  $U_{gr}(\psi)$ ,  $U_{in}(\psi)$ , and  $U_{tot}(\psi)$  for this case are shown in Fig. 6. We can determine the angle of deviation  $\theta$  of the pendulum from the horizontal line in any of the lateral equilibrium positions [ $\theta = \pi/2 - \psi_0$ , where  $\pm \psi_0$  are positions of the two symmetric minima of  $U_{tot}(\psi)$ , see Fig. 6] by equating the average value of the torque of the force of inertia tending to align the pendulum horizontally and the torque of the gravitational force tending to turn the pendulum downward into the vertical position:

$$\sin \theta = \frac{2gl}{a^2\omega^2}. \quad (15)$$

The lateral equilibrium positions exist if the product  $\omega a$  of the frequency and amplitude of horizontal vibration of the axis is greater than  $\sqrt{2gl}$ . Therefore the existence of these equilibrium positions at the horizontal vibration is deter-

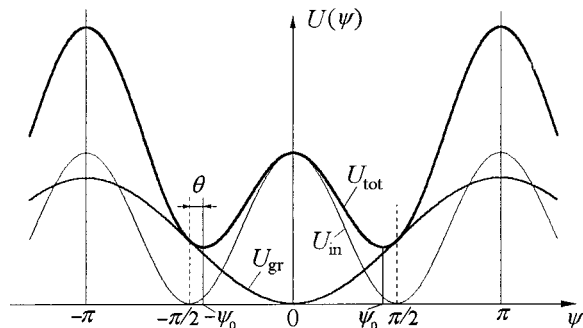


Fig. 6. Graphs of the gravitational potential energy  $U_{gr}$ , mean potential energy  $U_{in}$  in the field of the force of inertia, and of the total potential energy  $U_{tot}(\psi)$  for the pendulum with a horizontally oscillating axis.

mined by a criterion similar to condition (7) or (8) that determine stability of the inverted pendulum at vertical vibrations of the axis.

Both vertical positions correspond to an unstable equilibrium of the pendulum. If we gradually diminish the frequency  $\omega$  of forced horizontal oscillations of the axis or their amplitude  $a$  (or both  $\omega$  and  $a$ ), then, as we can see from Eq. (15), the angle  $\theta$  increases and the lateral stable equilibrium positions deviate more and more downward. They disappear at  $a^2\omega^2 \leq 2gl$  merging with the lower vertical equilibrium position, which then becomes stable.

An example of oscillations of the pendulum whose axis is driven with a high frequency in the horizontal direction is shown in Fig. 7. In its slow motion, the pendulum crosses several times the lower (unstable) vertical position, and eventually is captured in one of the lateral equilibrium positions. We can see that in the reference frame associated with the axis, after the slow motion has damped away, the pendulum's rod is not at rest but rather executes small rapid oscillations with the frequency of the axis. The final state in the phase plane is a small closed loop encircling the point that corresponds to the bottom of the effective potential well.

This behavior of the pendulum can also be easily demonstrated in a real experiment with the help of the simple device mentioned earlier. It is sufficient to turn it in the vertical plane through an angle of  $90^\circ$  in order for the pendulum's axis be forced to vibrate horizontally.

Computer simulations of similar oscillations about one of the lateral equilibrium positions in the absence of friction have been reported in Ref. 19.

## VI. MODES OF REGULAR SYNCHRONIZED OSCILLATIONS OF THE PARAMETRICALLY EXCITED PENDULUM

Next we briefly discuss the modes in which the driving frequency  $\omega$  is an integer multiple  $n$  of the frequency  $\omega_{up}$  (or  $\omega_{down}$ ) of slow oscillations:  $\omega = n\omega_{up}$  (or  $\omega = n\omega_{down}$ ). Over certain parts of the parameter space (the driving amplitude and frequency within certain ranges), the pendulum whose axis is vibrating with a high frequency, instead of gradually approaching the equilibrium position (either dynamically stabilized inverted position or ordinary downward position) by the process of damped slow oscillations, is trapped in an  $n$ -periodic oscillation locked in phase to the rapid oscillation of the axis. In such oscillations the phase trajectory repeats

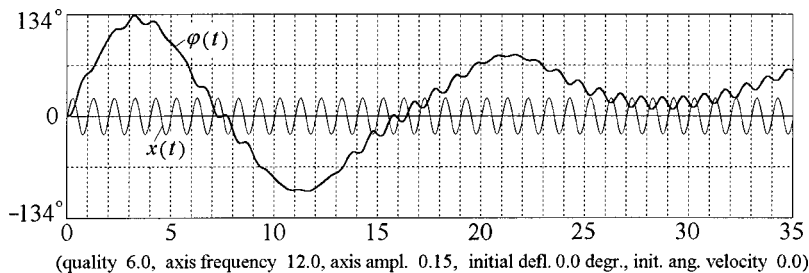


Fig. 7. The graph of damped oscillations of the pendulum whose axis is forced to rapidly vibrate in the horizontal direction. The graph is obtained by a numerical integration of the relevant exact differential equation for the momentary angular deflection  $\varphi(t)$ .

itself after  $n$  driving periods  $T$ . Since the motion has period  $nT$ , this phenomenon can be called a subharmonic resonance of  $n$ th order. An example of such stationary oscillations whose period equals eight periods of the axis is shown in Fig. 8. For the inverted pendulum with a vibrating pivot, periodic oscillations of this type were first described by Acheson,<sup>22</sup> who called them “multiple-nodding” oscillations.

The upper left-hand part of Fig. 8 shows the closed spatial trajectory of the pendulum’s bob at these “quadruple-nodding” oscillations. Such an extraordinary and even, at first sight, counterintuitive behavior of the pendulum can also be explained on the basis of the approximate approach developed earlier in Secs. II and III.

First of all we note that these modes of regular periodic oscillations are not specific to the inverted pendulum with a vibrating pivot. Similar oscillations can be executed also (at appropriate values of the driving parameters) about the ordinary (downward hanging) equilibrium position. Actually, the origin of these modes is independent of gravity, because such synchronized with the pivot “multiple-nodding” oscillations can occur also in the absence of gravity about any of the two equivalent dynamically stabilized equilibrium positions of the pendulum with a vibrating axis. Even the pendulum with horizontally vibrating pivot can execute similar  $n$ -periodic oscillations about each of the lateral equilibrium positions. Synchronization of these modes with the pivot oscillations creates conditions for supplying the energy to the pendulum needed to compensate for dissipation, and the whole process becomes exactly periodic.

The approximate theory developed earlier in this paper allows us to predict conditions at which these  $n$ -periodic oscillations can occur. For small amplitudes of the slow oscil-

lations, the corresponding minimum of the effective potential can be approximated by a parabolic well in which the smooth component of motion is almost harmonic. To estimate the frequency of this slow motion (the fundamental frequency), we can use Eq. (10). As an example, we next consider the pendulum in the absence of gravity, or, which is essentially the same, in the limiting case of very high driving frequencies  $\omega \gg \omega_0$  ( $\omega/\omega_0 \rightarrow \infty$ ). In this limit both equilibrium positions (ordinary and inverted) are equivalent, and the dimensionless driving amplitude  $a/l$  is the only parameter to be predicted as a required condition of the subharmonic resonance of order  $n$  (of synchronized with the pivot  $n$ -periodic oscillations of the pendulum).

According to Eq. (10), for  $\omega_0=0$  the frequency of slow oscillations is given by  $\omega_{\text{slow}}=a/(l\sqrt{2})\omega$ . For the “quadruple-nodding” mode the slow motion period equals eight periods of the axis, so that  $\omega_{\text{slow}}=\omega/8$ , whence  $a/l=\sqrt{2}/8=0.177$ . This value agrees well with the predictions of a more sophisticated quantitative theory of these modes based on the linearized differential equation of the system (see the Appendix), which gives for such period-8 small oscillations in the absence of gravity the following expression for the driving amplitude:  $a_{\text{min}}=63/(32\sqrt{130})l=0.173l$ . The latter value agrees perfectly with the simulation experiment in the limit of extremely small amplitudes.

Estimating conditions for  $n$ -periodic oscillations with the help of Eq. (10), we assume the slow motion of the pendulum in the effective potential well to be simple harmonic, which is true only if this motion is limited to within a small vicinity of the bottom of this well. Therefore we get the lower limit for the driving amplitude at which  $n$ -periodic oscillations of only infinitely small amplitude can occur.

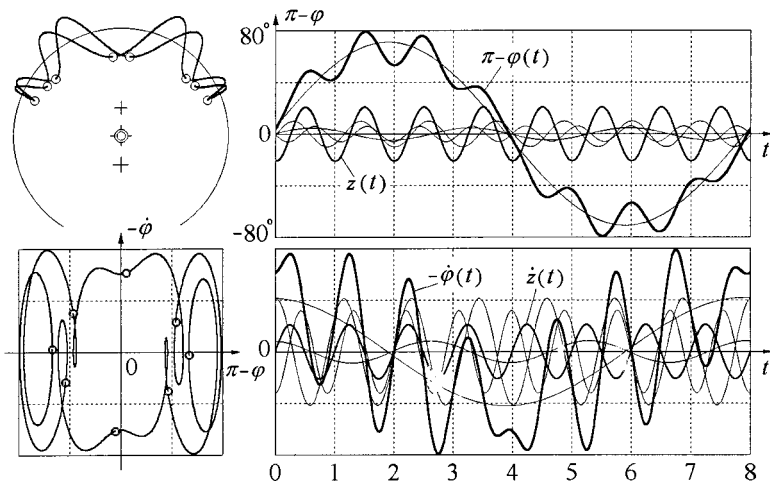
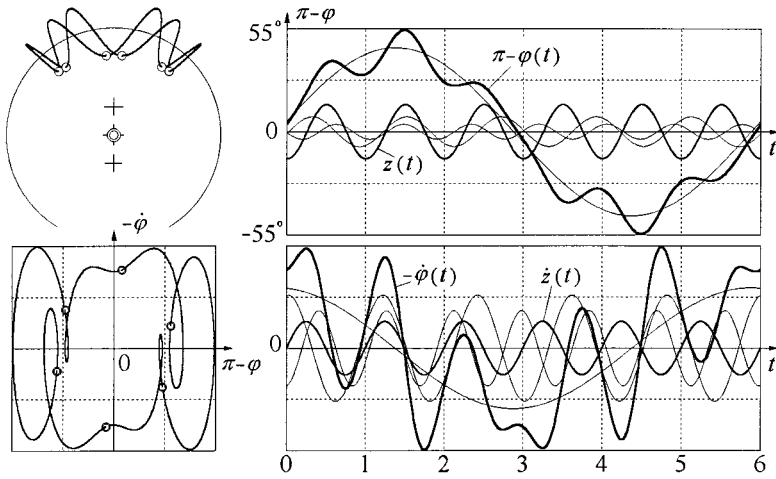


Fig. 8. The spatial path, phase orbit, and graphs of stationary oscillations with the period that equals eight periods of the oscillating axis. The graphs are obtained by a numerical integration of the exact differential equation for the momentary angular deflection  $\varphi(t)$ , Eq. (11).

(quality 400.0, no gravity, axis amplitude 0.265, initial defl. 175.51 degr., init. ang. velocity -0.2284)



(quality 400.0, no gravity, axis amplitude 0.265, initial defl. 175.77 degr., init. ang. velocity -0.1708)

Fig. 9. The spatial path, phase orbit, and graphs of stationary oscillations with the period that equals six periods of the oscillating axis. The graphs are obtained by a numerical integration of the exact differential equation for the momentary angular deflection  $\varphi(t)$ , Eq. (11).

Smooth nonharmonic oscillations of a finite angular excursion that extends over the slanting slopes of the nonparabolic effective potential well are characterized by a greater period than the small-amplitude harmonic oscillations occurring within the parabolic bottom of this well. Therefore large-amplitude period-8 oscillations shown in Fig. 8 (their swing equals  $80^\circ$ ) occur at a considerably greater value of the driving amplitude ( $a=0.265l$ ).

The right-hand side of Fig. 8, alongside the graphs of  $\varphi(t)$  and  $\dot{\varphi}(t)$  for the period-8 steady-state oscillations of the pendulum, shows also their harmonic components and the graphs of the pivot oscillations. The spectrum of these period-8 oscillations is rich in harmonics. The fundamental harmonic whose period equals eight driving periods dominates in the spectrum. We may treat it as a subharmonic (as an ‘‘undertone’’) of the driving oscillation. This principal harmonic describes the smooth component of the compound period-8 oscillation. Strange as it may seem from the first sight, the harmonic with the driving frequency has zero amplitude, that is, this harmonic is absent in the spectrum. However, this peculiarity also can be easily explained on the basis of the approach developed in this paper. In Eq. (3), which represents the angular position of the pendulum  $\varphi(t)$  as a superposition of slow and fast motions, the rapid component with the driving frequency enters the expression for  $\varphi(t)$  being multiplied by the sine of the slow varying coordinate  $\psi(t)$ . Therefore the rapid component has varying amplitude, which even changes its sign each time the pendulum crosses the equilibrium position. Actually, the rapidly oscillating second term in Eq. (3) is not a harmonic component in the spectrum of the resulting periodic oscillation, because harmonics of a periodic function are characterized by constant amplitudes.

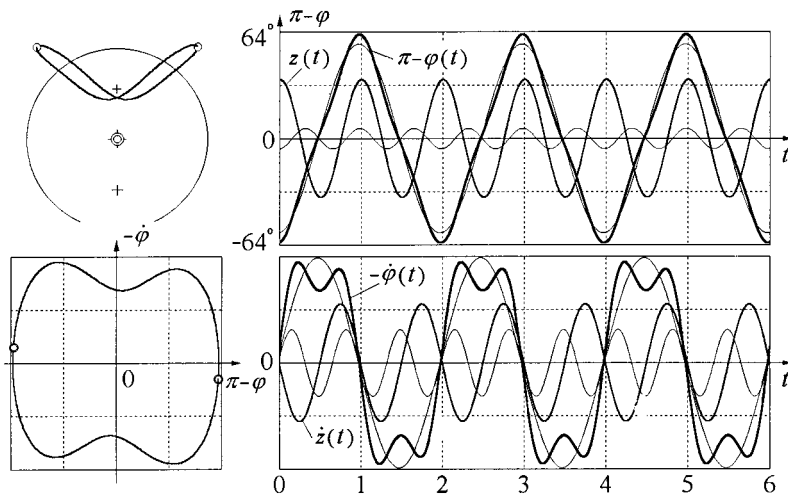
For small angular excursions of the pendulum occurring at driving amplitudes slightly greater than the critical value  $a_{\min}=0.173l$ , the spectrum of period-8 oscillations is formed by the principal harmonic (frequency  $\omega/8$ ), and also by the seventh and ninth harmonics whose frequencies ( $7\omega/8$  and  $9\omega/8$ ) are close to the driving frequency  $\omega$ . Their amplitudes equal, respectively, 11.3% and 6.8% of the principal harmonic amplitude. These theoretical values (see the Appendix) agree perfectly with the corresponding simulation experiment. For the oscillations of a large swing shown in Fig.

8, the amplitudes of these harmonics differ slightly from the above values, and the contributions of the third, fifth, and eleventh harmonics are also noticeable.

As noted earlier, in the case of period-8 oscillations of a small swing the approach based on the effective potential predicts for the driving amplitude  $a/l$  a value of  $\sqrt{2}/8=0.177$ , which is rather close to the exact low-amplitude theoretical limit ( $a/l=0.173$ ). To obtain the slow oscillations of a smaller period (say, of six driving periods), we should increase the driving amplitude. Indeed, when  $\omega_{\text{slow}}=\omega/6$ , Eq. (10) yields a greater value  $a/l=\sqrt{2}/6=0.236$ . However, for such period-6 oscillations this predicted value agrees somewhat worse with the theory based on the linearized equation of the system. This theory (see the Appendix) gives for period-6 small oscillations in the absence of gravity a value of the minimal driving amplitude of  $a_{\min}=35/(18\sqrt{74})l=0.226l$ , which perfectly agrees with the corresponding simulation experiment. Not surprisingly, for the  $n$ -periodic oscillation with a small  $n$  we cannot expect good quantitative predictions from the effective potential approach because in such cases the period of a ‘‘smooth’’ motion contains only a few driving periods. The ‘‘rapid’’ component of the motion here is not rapid enough for good averaging.

Nevertheless, the effective potential approach provides us not only with a qualitative understanding of these complex periodic modes, but also, being applicable to large-amplitude motions, explains the coexistence of several  $n$ -periodic modes with different  $n$  values at identical system parameters. Figure 9 shows large-amplitude period-6 asymptotic oscillations without gravity obtained at the same value  $a/l=0.265$  of the driving amplitude as the period-8 oscillations shown in Fig. 8.

For a large angular excursion, the smooth motion occurs in the nonparabolic effective potential well, in which the period becomes longer if we increase the amplitude. By virtue of this dependence of the period of nonharmonic smooth motion on the swing, different modes (modes with different values of  $n$ ) can coexist at the same amplitude of the pivot. Indeed, the period of a large-amplitude slow oscillation can be equal to, say, six driving periods, while the period of oscillation with a somewhat greater amplitude in the same nonparabolic potential well can be equal to eight driving



(quality 10.0, no gravity, axis amplitude 0.56, initial defl. 117.0 degr., init. ang. velocity 0.076)

Fig. 10. Stationary double-period oscillations occurring over the upper boundary of dynamic stability of the inverted pendulum. The graphs are obtained by a numerical integration of the exact differential equation for the momentary angular deflection  $\varphi(t)$ , Eq. (11).

periods. Figures 8 and 9 show, respectively, the simulations of such coexisting period-8 and period-6 modes, obtained at the identical parameters of the system. That is, both smooth motions occur in the same potential well. In which of these competing modes the pendulum eventually is trapped in a certain simulation, depends on the starting conditions. The set of initial conditions that leads, after an interval in which transients decay, to a given dynamic equilibrium (to the same steady-state periodic motion, or attractor) in the limit of large time, constitutes the basin of attraction of this attractor. The coexisting periodic motions in Figs. 8 and 9 represent competing attractors and are characterized by different domains of attraction.

With gravity, these complex  $n$ -periodic “multiple-nodding” modes exist both for the inverted and noninverted pendulums.

## VII. THE UPPER BOUNDARY OF THE DYNAMIC STABILITY

When the amplitude  $a$  of the pivot vibrations is increased beyond a certain critical value  $a_{\max}$ , the dynamically stabilized inverted position of the pendulum loses its stability. After a disturbance the pendulum does not come to rest in the up position, no matter how small the release angle, but instead eventually settles into a finite amplitude steady-state oscillation about the vertical position at frequency  $\omega/2$  (half the driving frequency). This loss of stability of the inverted pendulum has been first described by Blackburn *et al.*<sup>16</sup> (the “flutter” mode) and demonstrated experimentally in Ref. 17. The latest numerical investigation of the bifurcations associated with the stability of the inverted state can be found in Ref. 7. The graphs and the double-lobed phase trajectory of such oscillations are shown in Fig. 10.

Obviously, these oscillations can be regarded as a special case of the  $n$ -periodic steady-state modes considered in the previous section, particularly, the case that corresponds to  $n=2$ . As we already mentioned, for small values of  $n$  it is impossible to correctly represent the pendulum motion as consisting of the slow and rapid components. The driving amplitude  $a_{\max}$  is not small compared with the length  $l$  of the pendulum. Consequently, this case occurs beyond the limits of applicability of the approach based on the effective potential. This approach cannot explain the destabilization of the

inverted pendulum, as well as the loss of stability of the noninverted pendulum at conditions of ordinary parametric resonance. (In the latter case the driving amplitude can be small, but the driving frequency is not high enough for the separation of rapid and slow motions.)

However, the simulation shows (see Fig. 10) a very simple spectral composition of period-2 oscillations occurring over the upper boundary of dynamic stability: the fundamental harmonic whose frequency equals  $\omega/2$  (half the driving frequency  $\omega$ ) with a small addition of the third harmonic with the frequency  $3\omega/2$ . We note that large-amplitude oscillations of the noninverted pendulum in conditions of the principal parametric resonance are characterized by a similar spectrum. This similarity of the spectra is by no means occasional: Next we show that both the ordinary parametric resonance and the period-2 “flutter” mode that destroys the dynamic stability of the inverted state belong essentially to the same branch of possible steady-state period-2 oscillations of the parametrically excited pendulum. Therefore the upper boundary of dynamic stability for the inverted pendulum can be found directly from the differential equation of the system by the same method that is commonly used for determination of conditions which lead to the loss of stability of the noninverted pendulum through excitation of ordinary parametric resonance (the ranges of parametric instability; see, e.g., Ref. 10).

To calculate the critical driving amplitude that destabilizes the hanging down vertical position, we can replace  $\sin \varphi$  by  $\varphi$  in the exact differential equation of the parametrically driven pendulum, Eq. (11), and omit the damping term, thus reducing it to the Mathieu equation:

$$\ddot{\varphi} + \left( \omega_0^2 - \frac{a}{l} \omega^2 \sin \omega t \right) \varphi = 0. \quad (16)$$

Investigating stability of the inverted position, we use the (small) angle  $\theta = \pi - \varphi$ , and replace  $\sin \theta$  by  $\theta$  in the exact differential equation, Eq. (11). Thus we also obtain for the angle  $\theta$  of deflection from the inverted position the linear Mathieu equation which differs from Eq. (16) for the angle  $\varphi$  only by the opposite sign of the second term. As we can see clearly from Fig. 10, the periodic solution to this equation corresponding to the desired boundary of instability can be

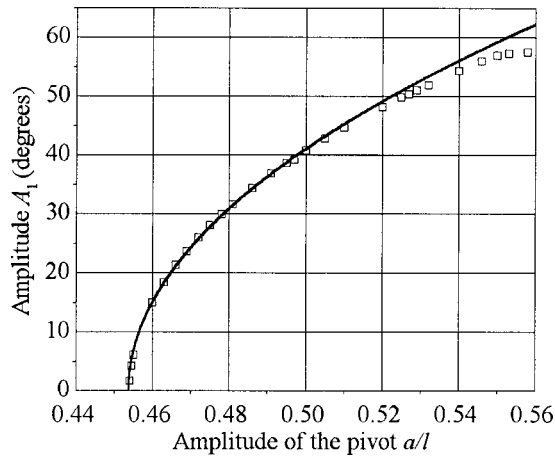


Fig. 11. The amplitude  $A_1$  of the principal harmonic for period-2 (“flutter”) steady-state oscillations of the pendulum over the upper boundary of the dynamic stability (in the absence of gravity).

sought as a superposition of the fundamental harmonic whose frequency  $\omega/2$  equals half the driving frequency, and the third harmonic with the frequency  $3\omega/2$ :

$$\theta(t) = \pi - \varphi(t) = A_1 \sin(\omega t/2) + A_3 \sin(3\omega t/2). \quad (17)$$

We consider first for simplicity the case  $\omega_0 = 0$ , which corresponds to the absence of gravity (or to the high frequency limit of the pivot oscillations with gravity). Substituting  $\theta(t)$  from Eq. (17) into the corresponding differential equation and expanding the products of trigonometric functions, we obtain an expression in which we should equate to zero the coefficients of  $\sin(\omega t/2)$  and  $\sin(3\omega t/2)$ . Thus we get a system of homogeneous equations for the coefficients  $A_1$  and  $A_3$ , which has a nontrivial solution when its determinant equals zero. This requirement yields a quadratic equation for the desired dimensionless critical driving amplitude  $a/l$ . The relevant root of this equation is  $a/l = 3(\sqrt{3} - 3)/4 = 0.454$ , and the corresponding ratio of amplitudes of the third harmonic to the fundamental one equals  $A_3/A_1 = (\sqrt{13} - 3)/6 = 0.101$ . A somewhat more complicated calculation in which the higher harmonics (up to the seventh) in  $\theta(t)$  are taken into account yields for  $a/l$  and  $A_3/A_1$  the values that coincide (within the assumed accuracy) with those cited above.

These values agree well with the simulation experiment in conditions of the absence of gravity ( $\omega_0 = 0$ ) and very small angular excursion of the pendulum. When the normalized amplitude of the pivot  $a/l$  exceeds the critical value  $a_{\max}/l = 0.454$ , the swing of the period-2 “flutter” oscillation (amplitude  $A_1$  of the fundamental harmonic) increases in proportion to the square root of this excess:  $A_1 \propto \sqrt{a - a_{\max}}$ . This dependence follows from the nonlinear differential equation of the pendulum, Eq. (11), if  $\sin \varphi$  in it is expanded as  $\varphi - \varphi^3/6$ , and also agrees well with the simulation experiment (Fig. 11) for amplitudes up to  $45^\circ$ .

As the amplitude  $a$  of the pivot is increased beyond the value  $0.555l$ , the symmetry-breaking bifurcation occurs: The angular excursions of the pendulum to one side and to the other become different, destroying the spatial symmetry of the oscillation and hence the symmetry of the phase orbit. As the pivot amplitude is increased further, after  $a/l = 0.565$  the system undergoes a sequence of period-doubling bifurca-

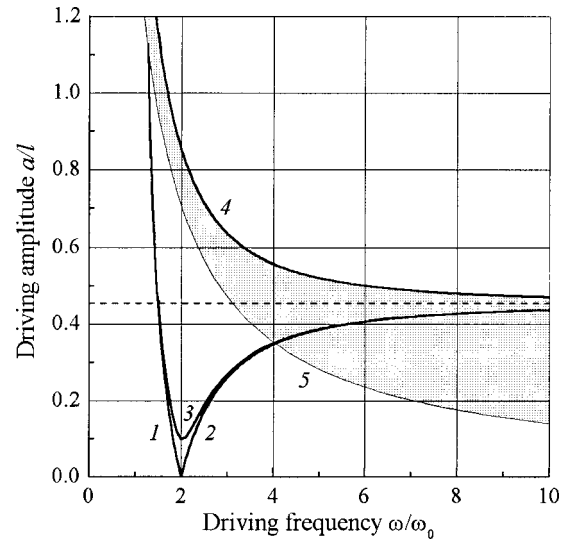


Fig. 12. The boundaries of parametric instability—driving amplitude vs normalized driving frequency. 1 and 2—left and right frequency boundaries of the principal interval of parametric instability ( $\omega \approx 2\omega_0$ ) for the noninverted pendulum in the absence of friction, 3—the same with friction ( $Q = 5.0$ ), 4 and 5—the upper and lower boundaries of dynamic stability for the inverted pendulum.

tions, and finally, at  $a/l = 0.56622$  (for  $Q = 20$ ), the oscillatory motion of the pendulum becomes replaced, at the end of a very long chaotic transient, by a regular unidirectional period-1 rotation.

Similar (though more complicated) theoretical investigation of the boundary conditions for period-2 stationary oscillations in the presence of gravity allows us to obtain the dependence of the critical (destabilizing) amplitude of the pivot on the driving frequency  $\omega$ . For the upper boundary of stability of the hanging down pendulum we find:

$$a/l = |(\sqrt{117 - 232(\omega_0/\omega)^2} + 80(\omega_0/\omega)^4 - 9 + 4(\omega_0/\omega)^2)/4, \quad (18)$$

and for the stability of the inverted pendulum:

$$a/l = (\sqrt{117 + 232(\omega_0/\omega)^2} + 80(\omega_0/\omega)^4 - 9 - 4(\omega_0/\omega)^2)/4. \quad (19)$$

The diagram in Fig. 12 shows these boundaries of instability.<sup>23</sup> For the hanging down pendulum, in the absence of friction the critical amplitude given by Eq. (18) tends to zero as the frequency of the pivot approaches  $2\omega_0$  from either side (curves 1 and 2). This case (small vertical oscillations of the pivot with the frequency approximately twice the natural frequency of the pendulum) corresponds to ordinary parametric resonance. Instability of the hanging down pendulum within the principal interval of parametric resonance allows a very clear physical explanation.<sup>24</sup> Curve 3 shows in the parameters plane  $(\omega/\omega_0, a/l)$  the region of principal parametric resonance with friction (for  $Q = 5.0$ ). The noninverted vertical position of the pendulum with the pivot vibrating at frequency  $2\omega_0$  loses stability when the normalized amplitude of this vibration exceeds the threshold value of  $1/2Q$ . This curve almost merges with curves 1 and 2 as the frequency  $\omega$  deviates from the resonant value  $2\omega_0$ . In the high-frequency limit, for which the role of gravity is negligible, the normalized critical pivot amplitude  $a/l$  tends to the

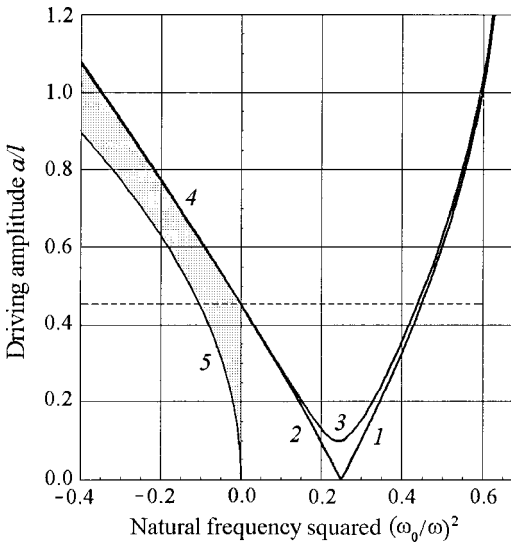


Fig. 13. The boundaries of parametric instability—driving amplitude vs natural frequency. 1 and 2—boundaries of the principal interval of parametric instability ( $\omega \approx 2\omega_0$ ) for the noninverted pendulum in the absence of friction, 3—the same with friction ( $Q=5.0$ ), 4 and 5—the upper and lower boundaries of dynamic stability for the inverted pendulum.

value indicated above,  $a/l = 3(\sqrt{13}-3)/4 = 0.454$ , that corresponds to the destabilization of the two symmetric equilibrium positions in the absence of gravity.

Curve 4 of this diagram given by Eq. (19) corresponds to destabilization of the inverted pendulum by excitation of the “flutter” oscillations. The smaller the frequency of the pivot, the greater the critical amplitude at which the inverted position becomes unstable. We note that this curve 4 for the boundary of the “flutter” mode is essentially the continuation (through infinite values of the driving frequency) of the same branch (curve 2 without friction or curve 3 with friction) of period-2 steady-state oscillations with the time dependence given by Eq. (17). That is, curve 4 is the continuation of curve 2 (or curve 3) that corresponds to the boundaries of instability with respect to excitation of the ordinary parametric resonance of the noninverted pendulum. This means that there is a close inherent relationship between the parametric instability of the noninverted pendulum (ordi-

nary parametric resonance) and the upper limit of the dynamic stability of the inverted pendulum (the “flutter” oscillations).

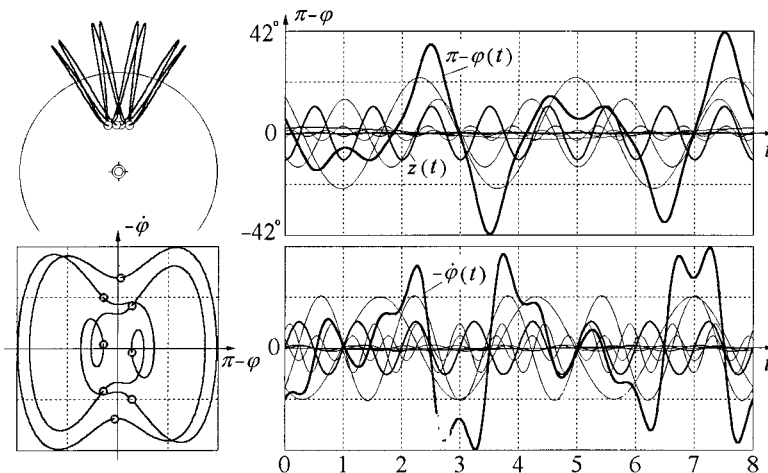
To make this relationship obvious, in Fig. 13 the same boundaries are shown as curves that give the dependence of the driving amplitude  $a/l$  on the inverse quantity  $(\omega_0/\omega)^2$  (instead of  $\omega/\omega_0$  in Fig. 12). We note that negative values of  $(\omega_0/\omega)^2$  correspond to the inverted pendulum, because the differential equation for the deviation from the inverted position  $\theta = \pi - \varphi$  differs from the differential equation for oscillations about the hanging downward position simply by the opposite sign of the term that describes the torque of gravitational and inertial forces. Curve 2 (or curve 3 in the presence of friction), which gives the boundary of ordinary parametric resonance for the noninverted pendulum, intersects the zero value of  $\omega_0/\omega$  (corresponding to an infinitely large driving frequency, or zero gravity) at  $a/l = 0.454$  and extends to the negative region of  $\omega_0/\omega$  as the upper boundary of stability for the inverted pendulum.

Curve 5 on both diagrams shows in the parameter plane the approximate lower boundary of dynamic stabilization of the inverted pendulum, given by Eq. (7) or Eq. (8). The loss of stability at crossing this lower boundary occurs when the effective potential well corresponding to the inverted position has zero depth. Thus, the region of stability of the inverted pendulum occupies the shaded part of the parameter plane between curves 5 and 4.

We note that complex  $n$ -periodic (or “multiple-nodding”) oscillations with  $n > 2$  (explained earlier in this paper on the basis of the effective potential approximation) occur at driving amplitudes  $a$  below the critical value  $a_{\max}$  and also occupy a region below curve 4 on the parameter plane. However, the existence of these asymptotic oscillatory states does not influence the dynamic stability of both inverted and ordinary equilibrium positions because the pendulum can be trapped in the  $n$ -periodic motions only after a certain initial disturbance, when its initial state occurs within the corresponding domain of attraction—otherwise the pendulum comes to rest.

## VIII. CONCLUDING REMARKS

The behavior of the parametrically excited pendulum discussed in this paper is richer in various modes than we can



(quality 60.0, axis frequency 5.0, axis ampl. 0.525, initial defl. 181.23 degr., init. ang. velocity 1.0477)

Fig. 14. The spatial path, phase orbit, and graphs of stationary oscillations with the period that equals eight periods of the oscillating axis. The graphs are obtained by a numerical integration of the exact differential equation for the momentary angular deflection  $\varphi(t)$ , Eq. (11).

expect for such a simple physical system relying on our intuition. Its nonlinear large-amplitude motions can hardly be called “simple.” The simulations show that variations of the parameter set (dimensionless driving amplitude  $a/l$ , normalized driving frequency  $\omega/\omega_0$ , and quality factor  $Q$ ) result in different regular and chaotic types of dynamical behavior.

One more example of rather counterintuitive regular oscillations is given by Fig. 14. The period of this motion equals eight driving periods, just like in the example shown in Fig. 8, but the character of oscillations and their spectrum differ dramatically. Here the third and fifth harmonics dominate in the spectrum. The third harmonic is characterized by an amplitude almost ten times greater than the fundamental harmonic.

In this paper we have touched only a small portion of the stationary states and regular motions of the parametrically excited pendulum. The pendulum’s dynamics exhibits a great variety of other asymptotic rotational, oscillatory, and combined (both rotational and oscillatory) multiple-periodic stationary states (attractors), whose basins of attraction are characterized by a surprisingly complex (fractal) structure. Computer simulations also reveal intricate sequences of bifurcations, leading to numerous intriguing chaotic regimes. All this remains beyond the scope of this paper. With good reason we can suppose that this apparently simple physical system is nearly inexhaustible.

## APPENDIX: SMALL-AMPLITUDE $n$ -PERIODIC OSCILLATIONS

To calculate the critical (minimal) driving amplitude that allows the pendulum to execute  $n$ -periodic stationary oscillations in the limit of small amplitudes (about both the hanging down and inverted positions), we can use the linearized differential equation of the parametrically driven pendulum, that is, the Mathieu equation, Eq. (16). We can search for its approximate small-amplitude solution  $\varphi(t)$  for period- $n$  oscillations as a superposition of the principal (fundamental) harmonic  $A_1 \sin(\omega t/n)$  whose frequency equals  $\omega/n$  (the subharmonic of order  $n$  with respect to the driving frequency  $\omega$ ), and a limited number of higher harmonics  $A_k \sin(k\omega t/n)$ . [Further on we chose the time origin so that the pivot’s motion is described by  $z(t) = a \cos \omega t$ .] Substituting  $\varphi(t)$  into the differential equation and expanding the products of trigonometric functions, we obtain a system of homogeneous equations for the coefficients  $A_k$  (for the amplitudes of harmonics). The homogeneous system has a nontrivial solution if its determinant equals zero. This condition yields an equation for the corresponding critical driving amplitude. Then, for the critical driving amplitude, the fractional amplitudes of different harmonics are found as the solutions to this homogeneous system of equations.

For the period-8 oscillations in the absence of gravity ( $\omega_0=0$ ), the procedure described above yields zero amplitudes of the third and fifth (and eleventh) harmonics. (However, Fig. 8 shows that for large angular excursions, for which the linearized differential equation is insufficient, the third harmonic also gives a noticeable contribution.) For the sake of simplicity we include here in the approximate solution only harmonics with significant (nonzero) amplitudes, specifically, the principal harmonic, and the seventh and ninth harmonics (which means that actually we ignore the contribution only of the thirteenth and all higher harmonics):

$$\varphi(t) = A_1 \cos(\omega t/8) + A_7 \cos(7\omega t/8) + A_9 \cos(9\omega t/8).$$

Substituting  $\varphi(t)$  in Eq. (16) with  $\omega_0=0$  yields the following system for  $A_n$ :

$$\begin{aligned} A_1 - 32(A_7 + A_9)(a/l) &= 0, & 32A_1(a/l) - 49A_7 &= 0, \\ 32A_1(a/l) - 81A_9 &= 0. \end{aligned}$$

A nontrivial solution exists for  $a/l = 63/(32\sqrt{130}) = 0.173$ . This critical value of the driving amplitude was already mentioned in Sec. VI, and it agrees exactly with the simulation experiment for period-8 small oscillations. The above equations also yield the fractional contributions of the seventh and ninth harmonics:  $A_7/A_1 = 9/(7\sqrt{130}) = 0.113$ ,  $A_9/A_1 = 7/(9\sqrt{130}) = 0.068$ —the values that also agree perfectly well with the simulations based on numerical integration of the differential equation.

Similarly, an approximate solution for the period-6 oscillations can be sought in the form:

$$\varphi(t) = A_1 \cos(\omega t/6) + A_5 \cos(5\omega t/6) + A_7 \cos(7\omega t/6),$$

which yields the following system of equations for  $A_n$ :

$$\begin{aligned} A_1 - 18(A_5 + A_7)(a/l) &= 0, & 18A_1(a/l) - 25A_5 &= 0, \\ 18A_1(a/l) - 49A_7 &= 0. \end{aligned}$$

These equations give for the critical driving amplitude the value  $a/l = 35/(18\sqrt{74}) = 0.226$ , and for fractional contributions of the fifth and seventh harmonics, respectively,  $A_5/A_1 = 7/(5\sqrt{74}) = 0.163$ , and  $A_7/A_1 = 5/(7\sqrt{74}) = 0.083$ . These theoretical values agree quite well with the simulations.

Similarly, for the period-4 small-amplitude oscillations:

$$\varphi(t) = A_1 \cos(\omega t/4) + A_3 \cos(3\omega t/4) + A_5 \cos(5\omega t/4),$$

$$\begin{aligned} A_1 - 8(A_3 + A_5)(a/l) &= 0, & 8A_1(a/l) - 9A_3 &= 0, \\ 8A_1(a/l) - 25A_5 &= 0, \end{aligned}$$

whence  $a/l = 15/(8\sqrt{34}) = 0.321$ ,  $A_3/A_1 = 5/(3\sqrt{34}) = 0.286$ ,  $A_5/A_1 = 3/(5\sqrt{34}) = 0.103$ . If in the approximate solution we also take into account the seventh harmonic, for zero gravity and zero friction we find more accurate values of the critical driving amplitude  $a/l = 0.320$  and fractional contributions of high harmonics  $A_3/A_1 = 0.288$ ,  $A_5/A_1 = 0.102$ ,  $A_7/A_1 = 0.015$ . We can compare these values with results of the simulation experiment:  $a/l = 0.320$ ,  $A_3/A_1 = 0.287$ ,  $A_5/A_1 = 0.101$ ,  $A_7/A_1 = 0.016$ .

The simulations show that, besides the above-considered  $n$ -periodic oscillations with even values of  $n$ , stationary parametric oscillations with odd  $n$  values ( $n=3,5,\dots$ ) are also possible. Critical values for the driving amplitudes that provide such small oscillations also can be found on the basis of a linearized theory, and the results of such calculations show good agreement with the simulations.

The existence of  $n$ -periodic subharmonic oscillations whose spectrum is characterized by zero (or very small) amplitude of the principal (fundamental) harmonic with frequency  $\omega/n$  may seem even more counterintuitive. An example of such period-8 oscillations is shown in Fig. 14. For small oscillations, third, fifth, and eleventh harmonics dominate in the spectrum, so that we can search an approximate solution of the linearized equation in the form:

$$\varphi(t) = A_3 \cos(3\omega t/8) + A_5 \cos(5\omega t/8) + A_{11} \cos(11\omega t/8).$$

Thus we find for the critical amplitude  $a/l = 165/(32\sqrt{146}) = 0.427$ , and for the fractional amplitudes of harmonics  $A_5/A_3 = 33/(5\sqrt{146}) = 0.546$ ,  $A_{11}/A_3 = 15/(11\sqrt{146}) = 0.113$ . More precise values (which agree well with the simulations) are obtained by including also the thirteenth harmonic:  $a/l = 0.419$ ,  $A_5/A_3 = 0.560$ ,  $A_{11}/A_3 = 0.111$ ,  $A_{13}/A_3 = 0.044$ .

Similar (though more complicated) calculations of the critical driving amplitudes and spectrum on the basis of a linearized differential equation are also possible for various modes of the parametrically driven pendulum in the presence of gravity and friction.

<sup>0</sup>Electronic mail: butikov@spb.runnet.ru

<sup>1</sup>Eugene Butikov, "The rigid pendulum—an antique but evergreen physical model," *Eur. J. Phys.* **20**, 429–441 (1999).

<sup>2</sup>John B. McLaughlin, "Period-doubling bifurcations and chaotic motion for a parametrically forced pendulum," *J. Stat. Phys.* **24** (2), 375–388 (1981).

<sup>3</sup>B. P. Koch, R. W. Leven, B. Pompe, and C. Wilke, "Experimental evidence for chaotic behavior of a parametrically forced pendulum," *Phys. Lett.* **96A** (5), 219–224 (1983).

<sup>4</sup>R. W. Leven, B. Pompe, C. Wilke, and B. P. Koch, "Experiments on periodic and chaotic motions of a parametrically forced pendulum," *Physica D* **16** (3), 371–384 (1985).

<sup>5</sup>Willem van de Water and Marc Hoppenbrouwers, "Unstable periodic orbits in the parametrically excited pendulum," *Phys. Rev. A* **44** (10), 6388–6398 (1991).

<sup>6</sup>John Starrett and Randall Tagg, "Control of a chaotic parametrically driven pendulum," *Phys. Rev. Lett.* **74** (11), 1974–1977 (1995).

<sup>7</sup>Sang-Yoon Kim and Bambi Hu, "Bifurcations and transitions to chaos in an inverted pendulum," *Phys. Rev. E* **58** (3), 3028–3035 (1998).

<sup>8</sup>A. Stephenson, "On an induced stability," *Philos. Mag.* **15**, 233–236 (1908).

<sup>9</sup>P. L. Kapitza, "Dynamic stability of the pendulum with vibrating suspension point," *Sov. Phys. JETP* **21** (5), 588–597 (1951) (in Russian); see also *Collected Papers of P. L. Kapitza*, edited by D. Ter Haar (Pergamon, London, 1965), Vol. 2, pp. 714–726.

<sup>10</sup>L. D. Landau and E. M. Lifschitz, *Mechanics* (Nauka, Moscow, 1988) (in Russian); *Mechanics* (Pergamon, New York, 1976), pp. 93–95.

<sup>11</sup>F. M. Phelps, III and J. H. Hunter, Jr., "An analytical solution of the inverted pendulum," *Am. J. Phys.* **33**, 285–295 (1965); **34**, 533–535 (1966).

<sup>12</sup>D. J. Ness, "Small oscillations of a stabilized, inverted pendulum," *Am. J. Phys.* **35**, 964–967 (1967).

<sup>13</sup>D. J. Acheson, "A pendulum theorem," *Proc. R. Soc. London, Ser. A* **443**, 239–245 (1993).

<sup>14</sup>H. P. Kalmus, "The inverted pendulum," *Am. J. Phys.* **38**, 874–878 (1970).

<sup>15</sup>M. M. Michaelis, "Stroboscopic study of the inverted pendulum," *Am. J. Phys.* **53** (11), 1079–1083 (1985).

<sup>16</sup>James A. Blackburn, H. J. T. Smith, and N. Groenbech-Jensen, "Stability and Hopf bifurcations in an inverted pendulum," *Am. J. Phys.* **60** (10), 903–908 (1992).

<sup>17</sup>H. J. T. Smith and J. A. Blackburn, "Experimental study of an inverted pendulum," *Am. J. Phys.* **60** (10), 909–911 (1992).

<sup>18</sup>Michael J. Moloney, "Inverted pendulum motion and the principle of equivalence," *Am. J. Phys.* **64** (11), 1431 (1996).

<sup>19</sup>W. T. Grandy, Jr. and Matthias Schöck, "Simulations of nonlinear pivot-driven pendula," *Am. J. Phys.* **65** (5), 376–381 (1997).

<sup>20</sup>Julia G. Fenn, Derek A. Bayne, and Bruce D. Sinclair, "Experimental investigation of the 'effective potential' of an inverted pendulum," *Am. J. Phys.* **66** (11), 981–984 (1998).

<sup>21</sup>P. S. Landa, *Nonlinear Oscillations and Waves in Dynamical Systems* (Kluwer, Dordrecht, 1996).

<sup>22</sup>D. J. Acheson, "Multiple-nodding oscillations of a driven inverted pendulum," *Proc. R. Soc. London, Ser. A* **448**, 89–95 (1995).

<sup>23</sup>A similar stability diagram for the parametrically driven pendulum is given by Fig. 4 of Ref. 16. The curves 2 and 3 of this diagram are given by the approximate equations  $a/l = 0.450 \mp 1.799(\omega_0/\omega)^2$  respectively, and tend to 0.450 in the limit of high driving frequencies (or zero gravity). However, the corresponding curves 2 and 4 in Fig. 12 of the present paper are given by exact equations, Eqs. (18) and (19). Approximate expansion of these equations for high driving frequencies yields  $a/l = 0.454 \mp 1.681(\omega_0/\omega)^2$ . Figure 12 also shows the lower-frequency boundary of parametric resonance (curve 1, or the left branch of curve 3 in the presence of friction), which is absent in Fig. 4 of Ref. 16.

<sup>24</sup>The time variations of the force of inertia give a clear physical explanation of the growth of initially small oscillations at conditions of parametric resonance. When the oscillating pivot is below its middle position, this additional force is directed downward, and vice versa. We can treat the effect of this varying force as a periodic modulation of the gravitational force. Let the pendulum move from the utmost deflection toward the lower equilibrium position while the pivot in its constrained oscillation is below the midpoint. Due to the additional apparent gravity the pendulum gains a greater speed than it would have gained in the absence of the pivot's motion. During the further motion of the pendulum away from the equilibrium position, the pivot is above its midpoint, so that the force of inertia reduces the apparent gravity. Thus the pendulum reaches a greater angular displacement than it would have reached otherwise. During the second half-period of the pendulum's motion the swing increases again, and so on, until the stationary motion is established due to violation of the resonance conditions at large swing.